Molecular theories of confined fluids

T. K. Vanderlick, L. E. Scriven, and H. T. Davis
Department of Chemical Engineering and Materials Science, University of Minnesota, Minneapolis, Minnesota 55455

(Received 4 May 1988; accepted 26 October 1988)

Density profiles and normal pressures predicted by three different approximate density functional free energy theories and the Fischer–Methfessel approximation to the Yvon–Born–Green (YBG) equation are compared with computer simulation results for fluids confined between planar walls. All models require as input a homogeneous fluid equation of state. Comparisons are made using two mean-field equations of state, one based on a Clausius hard-sphere reference fluid and the other based on a Carnahan/Starling hard-sphere reference fluid. The simplest and oldest of the models, the generalized van der Waals model, becomes unphysical at high mean pore densities. The Carnahan/Starling version of Tarazona model agrees best overall with the simulations. This model represents a systematic improvement on the generalized van der Waals model and is computationally the most complicated of all models examined. The YBG and generalized hard-rod models are not as accurate as the Tarazona model, but they capture the qualitative trends observed in the simulations. Both of these models are intuitive extensions of the exact theory of one-dimensional hard rods, and are computationally much simpler than the Tarazona model.

I. INTRODUCTION

Understanding the behavior of fluids confined by solid surfaces is of fundamental importance to many practical processes, such as lubrication, membrane separations, chromatography, adhesion, and enhanced oil recovery. Fluids confined by solid surfaces in at least one direction also play major roles in catalysis, drying of paper products, and aggregation of colloids. The behavior of confined fluids can be significantly different from that of bulk fluid. Furthermore, the properties of a confined fluid can vary dramatically with the degree of confinement.

The density distribution of a confined fluid can vary over multiple length scales. Layering and packing effects related to the finite size of the fluid particles cause the density to vary on a length scale the size of the fluid particles. Solid–fluid and fluid–fluid interactions can also give rise to thin-film structures whose length scales range from molecular to micron sizes. An example of the latter is wetting films sometimes present on solid surfaces.

One of the most demanding tests of theories of strongly inhomogeneous fluid, i.e., fluid whose density varies significantly over molecular dimensions, is the prediction of fluid structure between solid surfaces. The spatial arrangement of fluid particles is directly related to their ability to distribute themselves effectively in the gap between the solid surfaces. The theory must successfully account for the finite size of the fluid particles, which gives rise to the excluded volume effects that govern the equilibrium density distribution.

Free energy density functional theory is one common approach to predicting the density distribution of inhomogeneous fluid. The essence of free energy density functional theory is the construction of an expression for the free energy of the inhomogeneous system. This free energy is a functional of the density distribution, i.e., the variation of particle number density with position. This method originated with van der Waals,[1] who developed a mean-field theory of inhomogeneous fluid to predict the structure of the liquid–vapor interface. The rigorous, modern statistical mechanical foundations of density functional theory were largely laid a couple of decades ago.[2,3] Since then a lot of effort has gone into reducing the exact results to tractable but accurate approximations to describe liquid–vapor interfaces,[4–6] liquid–liquid interfaces,[7] wetting transitions at solid surfaces,[8,9] and solvation forces of fluid confined between solid surfaces.[10]

Parallel to the density functional free energy theory is the distribution function theory. The Yvon–Born–Green (YBG) equation, a prominent example of this theory, furnishes an exact relation between the density distribution $n(\mathbf{r})$ and the pair correlation function $g(\mathbf{r},\mathbf{r}')$. To render the rigorous YBG equation solvable for the fluid density distribution, an approximation of the inhomogeneous pair correlation function must be made. One such approximation was proposed by Fischer and Methfessel[11] and used successfully by them to "close" the YBG equation.

In this paper we explore the applicability of both types of theories to predicting the structure of confined fluid by examining the relative merits of the most prominent approximate free energy density functionals and the Yvon–Born–Green equation with the Fischer–Methfessel approximation. We apply for the first time a new free energy functional which was suggested by Robledo and Varea,[12] and also by Fischer and Heinbuch,[13] as a generalization of Percus' exact solution of the one-dimensional hard-rod system.[14] We focus on the ability of each model to predict density distributions when the average density of the confined fluid is high, similar to that of bulk liquid. Density distributions predicted by the various models are compared with available results from computer simulation.[15,16]

II. THEORY

In all that follows, it is assumed that the intermolecular potential $\Phi(\mathbf{r})$ can be divided into a purely hard-sphere po-

 0021-9606/89/042422-15$02.10

tential and an attractive potential:

$$\Phi(\mathbf{r}) = \Phi^{hs}(\mathbf{r}) + \Phi^{att}(\mathbf{r}), \tag{2.1}$$

where

$$\begin{aligned} \Phi^{hs}(\mathbf{r}) &= \infty, \quad |\mathbf{r}| < d, \\ &= 0, \quad |\mathbf{r}| \geqslant d, \end{aligned} \tag{2.2}$$

and d is the effective hard-sphere diameter.

The attractive part of the potential, $\Phi^{att}(\mathbf{r})$, is taken to be bounded and constant for $|\mathbf{r}| < d$; for $|\mathbf{r}| \geqslant d$ it is by construction equal to the total intermolecular potential $\Phi(\mathbf{r})$.

A. Free energy density functional theory

With the intermolecular potential defined as in Eq. (2.1), the classical Helmholz free energy F can be expressed as

$$F = F^{hs} + \Delta F^{att}, \tag{2.3}$$

where F^{hs} is the free energy of a hard-sphere reference fluid having the density distribution $n(\mathbf{r})$, and ΔF^{att} is the reversible work required to turn on all the attractive interactions without changing the density distribution.

In all the models studied here, it is assumed that ΔF^{att} can be estimated from the mean-field approximation, viz.,

$$\Delta F^{att} = \frac{1}{2}\int\int n(\mathbf{r})n(\mathbf{r}')g(\mathbf{r},\mathbf{r}')\Phi^{att}(|\mathbf{r}-\mathbf{r}'|)d^3r\,d^3r', \tag{2.4}$$

where $n(\mathbf{r})$ is the particle number density at position $\mathbf{r}$ and $g(\mathbf{r},\mathbf{r}')$ is the pair correlation function. In applying the models, we simplify the evaluation of Eq. (2.4) by introducing the structureless fluid approximation:

$$\begin{aligned} g(\mathbf{r},\mathbf{r}') &= 0, \quad |\mathbf{r}-\mathbf{r}'| < d, \\ &= 1, \quad |\mathbf{r}-\mathbf{r}'| \geqslant d. \end{aligned} \tag{2.5}$$

The free energy of the hard-sphere reference fluid is composed of a contribution arising from any external potentials acting on the fluid, an ideal gas piece, and an excess part, the latter accounting for departures from ideal gas behavior:

$$F^{hs} = F^{ext} + F^{ideal} + F^{excess}. \tag{2.6}$$

The excess hard-sphere free energy, F^{excess}, which has a major influence on the molecular structuring of the fluid, is not in general known. The external potential part and the ideal gas part of the free energy are

$$F^{ext} = \int n(\mathbf{r})u^{ext}(\mathbf{r})d^3r \tag{2.7}$$

and

$$F^{ideal} = kT\int n(\mathbf{r})[\ln n(\mathbf{r}) - 1]d^3r + N\mu^{\dagger}(T), \tag{2.8}$$

where $u^{ext}(\mathbf{r})$ is the external potential acting on a fluid particle at position $\mathbf{r}$, k is Boltzmann's constant, T is the temperature, and $\mu^{\dagger}(T)$ accounts for internal degrees of freedom of the molecules of the ideal gas. Because $\mu^{\dagger}(T)$ is related only to the datum of the chemical potential, we suppress it in what follows.

The equilibrium density distribution is that which minimizes the free energy subject to conservation of particles.[17] Equivalently, the equilibrium density distribution is an unconstrained minimum of the grand potential Ω where

$$\Omega = F - \mu\int n(\mathbf{r})d^3r. \tag{2.9}$$

Here, μ is the chemical potential [relative to the datum $\mu^{\dagger}(T)$] of the fluid. The equilibrium density profile is thus a solution to the following Euler–Lagrange equation for the minimization of Ω:

$$\mu = \frac{\delta F}{\delta n(\mathbf{r})}. \tag{2.10}$$

The direct correlation function $c(\mathbf{r},\mathbf{r}')$ is also directly related to the Helmholtz free energy:

$$c(\mathbf{r},\mathbf{r}') = \frac{-\delta^2[F - F^{ideal}]}{kT\delta n(\mathbf{r})\delta n(\mathbf{r}')} = \frac{-\delta^2 F^{excess}}{kT\delta n(\mathbf{r})\delta n(\mathbf{r}')}. \tag{2.11}$$

1. Helmholtz free energy: The generic model

Using one-dimensional hard-rod theory as an intuitive guide, Percus has defined a generic free energy functional for inhomogeneous hard-sphere fluids.[18] The free energy functional is built around an excess free energy that is a functional of two "coarse-grained" densities, $\bar{n}^{\sigma}(\mathbf{r})$ and $\bar{n}^{\tau}(\mathbf{r})$, which themselves are functionals of the local density distribution $n(\mathbf{r})$. His formula for the excess free energy is

$$F^{excess} = \int \bar{n}(\mathbf{r})\mathscr{F}_0[\bar{n}^{\tau}(\mathbf{r})]d^3r, \tag{2.12}$$

where $\mathscr{F}_0(n)$ is the excess free energy per particle of a *homogeneous* hard-sphere reference fluid of density n.

The coarse-grained densities $\bar{n}^{\sigma}(\mathbf{r})$ and $\bar{n}^{\tau}(\mathbf{r})$ are spatial averages of the local density over a small domain. Each coarse-grained density is defined by a weighting function which, in the most general case, is an explicit function of relative position and a functional of the density distribution:

$$\bar{n}^{\sigma}(\mathbf{r}) \equiv \int \sigma(\mathbf{r}-\mathbf{r}';\{n\})n(\mathbf{r}')d^3r', \tag{2.13}$$

$$\bar{n}^{\tau}(\mathbf{r}) \equiv \int \tau(\mathbf{r}-\mathbf{r}';\{n\})n(\mathbf{r}')d^3r'. \tag{2.14}$$

In homogeneous fluid, the local density is independent of position. In this case, each coarse-grained density reduces to the bulk density. This requires that the weighting functions be normalized at any given constant density, i.e.,

$$\int \sigma(\mathbf{r}-\mathbf{r}';n)d^3r' = \int \tau(\mathbf{r}-\mathbf{r}';n)d^3r' = 1. \tag{2.15}$$

The general expression for the excess hard-sphere free energy, Eq. (2.12), can be used to construct a generic free energy density functional, applicable to particles interacting with an intermolecular potential of the form given in Eq. (2.1). Reassembling the total Helmholtz free energy from the contributions given above [Eqs. (2.4), (2.7), (2.8), and

(2.12)] we obtain

$$F=\int n(\mathbf{r})u^{\mathrm{ext}}(\mathbf{r})d^3r+kT\int n(\mathbf{r})[\ln n(\mathbf{r})-1]d^3r$$
$$+\int \bar{n}^{\sigma}(\mathbf{r})\mathscr{F}_0[\bar{n}^{\tau}(\mathbf{r})]d^3r \qquad (2.16)$$
$$+\frac{1}{2}\int\int n(\mathbf{r})n(\mathbf{r}')\Phi^{\mathrm{att}}(|\mathbf{r}-\mathbf{r}'|)d^3r\,d^3r',$$

where we have redefined the attractive potential to be $\Phi^{\mathrm{att}}=0$ when $|\mathbf{r}-\mathbf{r}'|<d$, by virtue of the structureless fluid approximation used in ΔF^{att}.

The corresponding chemical potential, according to Eq. (2.10), is

$$\mu-u^{\mathrm{ext}}(\mathbf{r})=kT\ln n(\mathbf{r})+\int\frac{\delta\bar{n}^{\sigma}(\mathbf{r}')}{\delta n(\mathbf{r})}\mathscr{F}_0[\bar{n}^{\tau}(\mathbf{r}')]d^3r'$$
$$+\int\frac{\delta\bar{n}^{\tau}(\mathbf{r}')}{\delta n(\mathbf{r})}\bar{n}^{\sigma}(\mathbf{r}')\mathscr{F}_0'[\bar{n}^{\tau}(\mathbf{r}')]d^3r'$$
$$+\int n(\mathbf{r}')\Phi^{\mathrm{att}}(|\mathbf{r}-\mathbf{r}'|)d^3r', \qquad (2.17)$$

where $\delta\bar{n}(\mathbf{r}')/\delta n(\mathbf{r})$ is the functional derivative of the coarse-grained density ($\bar{n}^{\sigma}$ or $\bar{n}^{\tau}$) with respect to the local density. $\mathscr{F}_0'(n)$ is the derivative of $\mathscr{F}_0(n)$ with respect to density.

To complete the theory, the exact forms of the weighting functions σ and τ must be established. Also, the excess free energy per particle of the homogeneous hard-sphere reference fluid $\mathscr{F}_0$ must be specified. Then, for a given chemical potential, temperature, external potential, and intermolecular potential, the equilibrium density distribution is a solution of Eq. (2.17).

The assignment of weighting functions generates different model density functionals, such as the van der Waals model, the generalized van der Waals model, etc. These are described in what follows. Specific versions of each model are generated by the equation of state used to determine the excess free energy of the homogeneous hard-sphere reference fluid.

One of the simplest hard-sphere equations of state that can be used to generate the thermodynamic properties of the hard-sphere reference fluid is the Clausius equation of state:

$$P_0^{\mathrm{hs}}=kTn/(1-nb), \qquad (2.18)$$

where P_0^{hs} is the pressure of the hard-sphere fluid and b is the excluded volume per particle. The excess hard-sphere free energy per particle derived from this equation of state is

$$\mathscr{F}_0(n)=kT\ln\left(\frac{1}{1-nb}\right). \qquad (2.19)$$

Alternatively, the Carnahan/Starling equation[19] is known to be quite accurate for hard-sphere fluids. It is given by

$$P_0^{\mathrm{hs}}=kT\frac{1+y+y^2-y^3}{(1-y)^3},\quad y\equiv\frac{\pi nd^3}{6}. \qquad (2.20)$$

The corresponding excess free energy per particle is

$$\mathscr{F}_0(n)=kT\frac{y(4-3y)}{(1-y)^2}. \qquad (2.21)$$

The equation of state of homogeneous fluid dictated by the generic free energy functional given in Eq. (2.16) is independent of the choice of weighting functions. The pressure of homogeneous fluid is composed of a hard-sphere pressure, given by the equation of state used to model the hard-sphere reference fluid, and a mean-field attractive contribution:

$$P_0=P_0^{\mathrm{hs}}+\frac{n^2}{2}\int\Phi^{\mathrm{att}}(|\mathbf{r}|)d^3r. \qquad (2.22)$$

The chemical potential (relative to the datum $\mu^{\dagger}$) in homogeneous fluid given by this mean-field equation of state is

$$\mu=kT\ln n+\mathscr{F}_0(n)+n\mathscr{F}_0'(n)+n\int\Phi^{\mathrm{att}}(|\mathbf{r}|)d^3r. \qquad (2.23)$$

Equations (2.22) and (2.23) rest on the earlier assignment: $\Phi^{\mathrm{att}}(|\mathbf{r}|)=0$, for $|\mathbf{r}|<d$.

An important point is that the particle number density $n(\mathbf{r})$ can be interpreted as the probability of finding the center of a particle at position $\mathbf{r}$. In homogeneous fluid, this density is a constant, independent of position. For a given equation of state, the homogeneous fluid density can be no larger than the density at close packing, i.e., the density at which the pressure diverges. A mean-field equation of state, Eq. (2.22), based on the Clausius hard-sphere equation of state, Eq. (2.18), cannot predict a homogeneous density greater than $1/b$, where b is the excluded volume per particle. Equations of state based on the Carnahan/Starling hard-sphere equation of state cannot predict a homogeneous density greater than $(6/\pi)d^{-3}$.

In an inhomogeneous fluid, the local density can take on values much higher than the close-packed limit. In other words, the probability that the center of a particle is located at certain positions can be very high, approaching infinity in a perfectly ordered crystalline material. According to the generic free energy functional, Eq. (2.16), the close-packed density limit in inhomogeneous fluid must be obeyed not by the local density, but rather by the coarse-grained density $\bar{n}^{\tau}(\mathbf{r})$.

2. The van der Waals model

The original free energy density functional model of van der Waals[1] is a particular case of the generic free energy functional given by Eq. (2.16). In this particular case, the weighting functions are

$$\sigma(\mathbf{r})=\tau(\mathbf{r})\equiv\delta(\mathbf{r}), \qquad (2.24)$$

where $\delta(\mathbf{r})$ is the Dirac delta function. Thus, both coarse-grained densities $\bar{n}^{\tau}(\mathbf{r})$ and $\bar{n}^{\sigma}(\mathbf{r})$ reduce to the local density $n(\mathbf{r})$. Hence, the free energy, as well as the chemical potential, depends only on the local point densities.

The chemical potential is given by

$$\mu-u^{\mathrm{ext}}(\mathbf{r})=kT\ln n(\mathbf{r})+\mathscr{F}_0[n(\mathbf{r})]+n(\mathbf{r})\mathscr{F}_0'[n(\mathbf{r})]$$
$$+\int n(\mathbf{r}')\Phi^{\mathrm{att}}(|\mathbf{r}-\mathbf{r}'|)d^3r'. \qquad (2.25)$$

Because it neglects the nonlocal contributions arising from the finite of size of the particles, the van der Waals model

fails to predict, even qualitatively, the structure of fluids next to or between solid surfaces. Thus, we shall not consider it further.

3. The generalized van der Waals model

The generalized van der Waals model of Nordholm and co-workers[20,21] was the first free energy density functional model to incorporate a nonlocal coarse-grained density. This model can be cast in the generalized form given by Eq. (2.16). The weighting functions of the generalized van der Waals model are

$$\sigma(\mathbf{r}) \equiv \delta(\mathbf{r}), \tag{2.26}$$

$$\tau(\mathbf{r}) \equiv H(d - |\mathbf{r}|) \Big/ \left(\frac{4\pi d^3}{3}\right), \tag{2.27}$$

where $H(r)$ is the Heaviside step function:

$$\begin{aligned} H(r) &= 1, \quad r \geqslant 0, \\ &= 0, \quad r < 0. \end{aligned} \tag{2.28}$$

The range of the nonlocal weighting function τ is the effective hard-sphere diameter d. The coarse-grained density $\bar{n}^{\tau}(\mathbf{r})$ represents the average density in a sphere of *radius d* about $\mathbf{r}$; $\bar{n}^{\sigma}(\mathbf{r})$ is equal to the local density $n(\mathbf{r})$.

The chemical potential is given by

$$\begin{aligned} \mu - u^{\text{ext}}(\mathbf{r}) = kT \ln n(\mathbf{r}) &+ \mathscr{F}_0[\bar{n}^{\tau}(\mathbf{r})] \\ &+ \int H(d - |\mathbf{r} - \mathbf{r}'|) n(\mathbf{r}') \mathscr{F}_0'[\bar{n}^{\tau}(\mathbf{r}')] d^3r' \\ &+ \int n(\mathbf{r}') \Phi^{\text{att}}(|\mathbf{r} - \mathbf{r}'|) d^3r'. \end{aligned} \tag{2.29}$$

Specific versions of the generalized van der Waals model are based on different equations of state for the hard-sphere reference fluid. In their original development, Nordholm *et al.*[20] used the Clausius expression for $\mathscr{F}_0$, Eq. (2.19), with the excluded volume parameter b equal to d^3. They also put forward[20] a Clausius version of the generalized van der Waals model with a density dependent excluded volume parameter which is interpolated between the low density limit of $\frac{2}{3}\pi d^3$ and the high density cubic close-packed limit of d^3. Tarazona and co-workers,[22] as well as Hooper and Nordholm,[23] have developed a version of the generalized van der Waals model that is based on the Carnahan/Starling equation of state.

It turns out that at some chemical potentials Eq. (2.29) admits for the Clausius formula for $\mathscr{F}_0$ solutions that have regions of negative density.[24] These are, of course, nonphysical solutions. The alternative to finding an equilibrium solution from the generalized van der Waals model is to find the density distribution that minimizes Eq. (2.9) subject to the constraint $n(x) \geqslant 0$. We do not pursue this approach here. In what follows we present only the unconstrained solutions to Eq. (2.29).

4. The generalized hard-rod model

The density distribution of one-dimensional hard rods in an external potential is known[14] and can be solved for analytically.[25] Percus[18] has shown that the solution of Eq. (2.17), with $\Phi^{\text{att}} = 0$, is the exact density distribution of one-dimensional hard rods when the weighting functions are

$$\sigma(x) \equiv \delta\left(\frac{d}{2} - |x|\right) \Big/ 2, \tag{2.30}$$

$$\tau(x) \equiv H\left(\frac{d}{2} - |x|\right) \Big/ d. \tag{2.31}$$

Robledo and Varea,[12] and also Fischer and Heinbuch,[13] have developed a free energy density functional model based on weighting functions which are generalizations of these one-dimensional weighting functions to three dimensions. This model, termed here the generalized hard-rod model, is characterized by the following weighting functions, $\sigma(\mathbf{r})$ and $\tau(\mathbf{r})$:

$$\sigma(\mathbf{r}) \equiv \delta\left(\frac{d}{2} - |r|\right) \Big/ \left[4\pi \left(\frac{d}{2}\right)^2\right], \tag{2.32}$$

$$\tau(\mathbf{r}) \equiv H\left(\frac{d}{2} - |r|\right) \Big/ \left[\frac{4\pi}{3} \left(\frac{d}{2}\right)^3\right]. \tag{2.33}$$

The chemical potential μ is thus

$$\begin{aligned} \mu - u^{\text{ext}}(\mathbf{r}) = kT \ln n(\mathbf{r}) &+ \frac{1}{4\pi(d/2)^2} \int \delta\left(|\mathbf{r} - \mathbf{r}'| - \frac{d}{2}\right) \mathscr{F}_0[\bar{n}^{\tau}(\mathbf{r}')] d^3r' \\ &+ \frac{1}{(4\pi/3)(d/2)^3} \int H\left(\frac{d}{2} - |\mathbf{r} - \mathbf{r}'|\right) \bar{n}^{\sigma}(\mathbf{r}') \mathscr{F}_0'[\bar{n}^{\tau}(\mathbf{r}')] d^3r' + \int n(\mathbf{r}') \Phi^{\text{att}}(|\mathbf{r} - \mathbf{r}'|) d^3r'. \end{aligned} \tag{2.34}$$

5. The Tarazona model

The free energy theories described thus far are built upon nonlocal densities defined by weighting functions that depend on relative position alone. Another approach developed by Tarazona,[26] is to incorporate a nonlocal density defined by a *density weighted* spatial average of the local density. Although others have also developed free energy functionals based on this premise,[27,28] we examine only the one proposed by Tarazona; the others make computation more complicated.

Tarazona's free energy functional can be cast in the general form given by Eq. (2.16). Like its predecessor, the generalized van der Waals model, Tarazona's free energy functional is based on only one nonlocal density $\bar{n}^{\tau}(\mathbf{r})$. The first weighting function $\sigma(\mathbf{r})$ is equal to the Dirac delta function, so that $\bar{n}^{\sigma}(\mathbf{r})$ reduces to the local density $n(\mathbf{r})$. However, unlike the free energy models discussed so far, the nonlocal

weighting function τ is a functional of the density distribution. Specifically $\bar{n}^{\tau}(\mathbf{r})$ is expressed in terms of a weighting function which depends explicitly on relative position and on $\bar{n}^{\tau}(\mathbf{r})$, and is given by the following integral equation:

$$\bar{n}^{\tau}(\mathbf{r}) = \int \tau\,[\mathbf{r}-\mathbf{r}';\bar{n}^{\tau}(\mathbf{r})]\,n(\mathbf{r}')\,d^3r'. \tag{2.35}$$

Tarazona expresses the density dependent weighting function as a series in the nonlocal density; the series is in practice truncated after the third term:

$$\tau[\mathbf{r}-\mathbf{r}';\bar{n}^{\tau}(\mathbf{r})] \equiv \omega_0(|\mathbf{r}-\mathbf{r}'|) + \omega_1(|\mathbf{r}-\mathbf{r}'|)\bar{n}^{\tau}(\mathbf{r}) + \omega_2(|\mathbf{r}-\mathbf{r}'|)\bar{n}^{\tau}(\mathbf{r})^2. \tag{2.36}$$

With τ defined in this fashion, $\bar{n}^{\tau}(\mathbf{r})$ can be expressed in terms of three other nonlocal densities, $\bar{n}_0(\mathbf{r})$, $\bar{n}_1(\mathbf{r})$, and $\bar{n}_2(\mathbf{r})$, that are defined by density-independent weighting functions, $\omega_0(\mathbf{r})$, $\omega_1(\mathbf{r})$, and $\omega_2(\mathbf{r})$, respectively:

$$\bar{n}^{\tau}(\mathbf{r}) \equiv \bar{n}_0(\mathbf{r}) + \bar{n}_1(\mathbf{r})\bar{n}^{\tau}(\mathbf{r}) + \bar{n}_2(\mathbf{r})\bar{n}^{\tau}(\mathbf{r})^2, \tag{2.37}$$

where

$$\bar{n}_i(\mathbf{r}) \equiv \int \omega_i(|\mathbf{r}-\mathbf{r}'|)\,n(\mathbf{r}')\,d^3r', \quad i=0,1,2. \tag{2.38}$$

The density-independent weighting functions have the properties

$$\int \omega_i(|\mathbf{r}|)\,d^3r = 1, \quad i=0, \qquad = 0, \quad i=1,2 \tag{2.39}$$

which follow from the normalization condition of τ, Eq. (2.15).

The criterion used to specify the exact forms of the spatial weighting functions $\omega_i(\mathbf{r})$ is given by requiring close agreement, over a range of densities, of the direct correlation function calculated from Eq. (2.11) with that predicted by the Percus–Yevick approximation for a homogeneous hard-sphere fluid. To accomplish this, Tarazona prescribes algebraic expressions for the density-independent weighting functions (presented without typographical errors in Ref. 29):

$$\omega_0(|\mathbf{r}|) \equiv \left(\frac{3}{4\pi d^3}\right), \quad |\mathbf{r}|<d, \qquad \equiv 0, \quad |\mathbf{r}|>d, \tag{2.40a}$$

$$\omega_1(|\mathbf{r}|) \equiv 0.475 - 0.648\left(\frac{|\mathbf{r}|}{d}\right) + 0.113\left(\frac{|\mathbf{r}|}{d}\right)^2, \quad |\mathbf{r}|<d,$$
$$\equiv 0.288\left(\frac{d}{|\mathbf{r}|}\right) - 0.924 + 0.764\left(\frac{|\mathbf{r}|}{d}\right) - 0.187\left(\frac{|\mathbf{r}|}{d}\right)^2, \quad d<|\mathbf{r}|>2d, \tag{2.40b}$$
$$\equiv 0, \quad |\mathbf{r}|>2d,$$

$$\omega_2(|\mathbf{r}|) \equiv \frac{5\pi d^3}{144}\left[6 - 12\left(\frac{|\mathbf{r}|}{d}\right) + 5\left(\frac{|\mathbf{r}|}{d}\right)^2\right], \quad |\mathbf{r}|<d, \qquad \equiv 0, \quad |\mathbf{r}|>d. \tag{2.40c}$$

Tarazona obtained these weighting functions for a free energy model based on the Carnahan/Starling hard-sphere equation of state, Eq. (2.20), and so they are consistent only with that particular version of the model. Nevertheless these same expressions can be used with the Tarazona model based on the Clausius hard-sphere equation of state, Eq. (2.19); this we do here with the excluded volume equal to d^3.

The chemical potential is given by

$$\mu - u^{\text{ext}}(\mathbf{r}) = kT\ln n(\mathbf{r}) + \mathscr{F}_0[\bar{n}^{\tau}(\mathbf{r})] + \int \frac{\delta\bar{n}^{\tau}(\mathbf{r}')}{\delta n(\mathbf{r})}\,n(\mathbf{r}')\,\mathscr{F}_0'[\bar{n}^{\tau}(\mathbf{r}')]\,d^3r' + \int n(\mathbf{r}')\,\Phi^{\text{att}}(|\mathbf{r}-\mathbf{r}'|)\,d^3r', \tag{2.41}$$

where

$$\frac{\delta\bar{n}^{\tau}(\mathbf{r}')}{\delta n(\mathbf{r})} = \frac{\tau[\mathbf{r}'-\mathbf{r};\bar{n}^{\tau}(\mathbf{r}')]}{1-\bar{n}_1(\mathbf{r}')-2\bar{n}_2(\mathbf{r}')\bar{n}^{\tau}(\mathbf{r}')}. \tag{2.42}$$

The coarse-grained density $\bar{n}^{\tau}(\mathbf{r})$ is a root of the quadratic equation, Eq. (2.37). The physically appropriate root is

$$\bar{n}^{\tau}(\mathbf{r}) = \frac{[1-\bar{n}_1(\mathbf{r})] - \{[1-\bar{n}_1(\mathbf{r})]^2 - 4\bar{n}_0(\mathbf{r})\bar{n}_2(\mathbf{r})\}^{1/2}}{2\bar{n}_2(\mathbf{r})}. \tag{2.43}$$

When the density does not vary greatly over length scales of order d, the hard-sphere diameter, the density-dependent weighting function τ reduces to the density-independent weighting function ω_0. Furthermore, this weighting function is the same as the one used in the generalized van der Waals model.

B. Yvon–Born–Green theory: The Fischer–Methfessel model

The Yvon–Born–Green (YBG) equation relates the local number density $n(\mathbf{r})$ to the pair correlation function $g(\mathbf{r},\mathbf{r}')$. With the intermolecular potential defined as in Eq.

(2.1), the YBG equation becomes[30,31]

$$kT\nabla \ln n(\mathbf{r}) = -\nabla u^{\text{ext}}(\mathbf{r}) - \int n(\mathbf{r}')g(\mathbf{r},\mathbf{r}')\nabla\Phi^{\text{att}}(|\mathbf{r}-\mathbf{r}'|)d^3r' - kT\int n(\mathbf{r}')g(\mathbf{r},\mathbf{r}')\nabla\Phi^{\text{hs}}(|\mathbf{r}-\mathbf{r}'|)d^3r'. \quad (2.44)$$

Following the development of Fischer and Methfessel,[11] we make two simplifying approximations. First, as with the free energy models, the structureless fluid approximation can be used in evaluating the attractive force average. Next, the correlation function in the second integral can be replaced by the correlation function of a purely hard-sphere reference fluid, $g(\mathbf{r},\mathbf{r}')\approx g^{\text{hs}}(\mathbf{r},\mathbf{r}')$. With these simplifying approximations, the YBG equation can be rearranged to

$$kT\nabla \ln n(\mathbf{r}) = -\nabla u^{\text{ext}}(\mathbf{r}) - \nabla\int n(\mathbf{r}')\Phi^{\text{att}}(|\mathbf{r}-\mathbf{r}'|)d^3r' - kT\int n(\mathbf{r}')g^{\text{hs}}(\mathbf{r},\mathbf{r}';|\mathbf{r}-\mathbf{r}'|=d)\times\frac{(\mathbf{r}-\mathbf{r}')}{|\mathbf{r}-\mathbf{r}'|}\delta(|\mathbf{r}-\mathbf{r}'|-d)d^3r'. \quad (2.45)$$

The pair correlation function of the hard-sphere reference system is evaluated only at contact, i.e., at $|\mathbf{r}-\mathbf{r}'|=d$.

The pair correlation function for an inhomogeneous system of hard spheres cannot be expressed in closed form. It can be written in terms of three-body correlations through the Born–Green–Yvon hierarchy,[29,30] but if a usable result is to be obtained, this hierarchy of equations must eventually be "closed" at the $(n-1)$st level by an approximation of the nth correlation function.

In the Fischer–Methfessel approximation, the inhomogeneous pair correlation function is replaced by a pair correlation function of homogeneous fluid, evaluated at a coarse-grained density $\bar{n}(\mathbf{r})$:

$$g^{\text{hs}}(\mathbf{r},\mathbf{r}';|\mathbf{r}-\mathbf{r}'|=d)\approx g_0^{\text{hs}}\left[|\mathbf{r}-\mathbf{r}'|=d,\bar{n}\left(\frac{\mathbf{r}+\mathbf{r}'}{2}\right)\right]. \quad (2.46)$$

For the coarse-grained density $\bar{n}(\mathbf{r})$, they chose a spatial average of the local density over a sphere of *diameter* equal to the hard-sphere diameter d centered at the point of contact, $(\mathbf{r},\mathbf{r}')/2$:

$$\bar{n}(\mathbf{r})\equiv\int\omega(|\mathbf{r}-\mathbf{r}'|)n(\mathbf{r}')d^3r', \quad (2.47)$$

where

$$\omega(|\mathbf{r}-\mathbf{r}'|)\equiv H\left(\frac{d}{2}-|\mathbf{r}-\mathbf{r}'|\right)\Big/\left[\frac{4\pi}{3}\left(\frac{d}{2}\right)^3\right]. \quad (2.48)$$

Thus, $\bar{n}(\mathbf{r})$ is the same as the coarse-grained density $\bar{n}^{\tau}(\mathbf{r})$ introduced in the generalized hard-rod model.

The homogeneous pair correlation function of hard spheres, evaluated at contact, is needed to complete the YBG theory. Fischer and Methfessel[11] used the Carnahan/Starling hard-sphere equation of state to approximate the homogeneous pair correlation function. The result is

$$g_0^{\text{hs}}(d,n)=\frac{1-(\pi/12)nd^3}{[1-(\pi/6)nd^3]^3}. \quad (2.49)$$

To recover the Clausius equation of state, one uses a hard-sphere pair correlation function of the form

$$g_0^{\text{hs}}(d,n)=\frac{2b/(4\pi d^3/3)}{1-nb}, \quad (2.50)$$

where b is the excluded volume per particle. In analogy with free energy models based on the Clausius hard-sphere equation of state, we set $b=d^3$ in the calculations presented below.

III. ONE-DIMENSIONAL HARD RODS IN AN EXTERNAL POTENTIAL

A benchmark for comparison of all theories is the prediction of the density distribution of one-dimensional hard rods in an external potential. The density distribution and thermodynamic properties of this system are known rigorously,[14] essentially because excluded volume effects in one dimension can be exactly determined.

The excess free energy per particle of a homogeneous system of hard rods is

$$\mathscr{F}_0(n)=kT\ln\left(\frac{1}{1-nd}\right). \quad (3.1)$$

By construction, the generalized hard-rod model reduces in one-dimension to the rigorous free energy density functional of hard rods.

Davis has shown[32] that the YBG equation with the Fischer–Methfessel approximation of the pair correlation function is also exact in one dimension.

The generalized van der Waals theory is not exact in one dimension. In one dimension, the three-dimensional weighting functions given by Eqs. (2.26) and (2.27) become

$$\sigma(x)=\delta(x) \quad (3.2)$$

and

$$\tau(x)=H(d-|x|)/(2d). \quad (3.3)$$

IV. APPLICATION TO FLUIDS CONFINED IN SLIT PORES

The theories presented in Sec. II can be used to predict the density distribution of fluid confined between planar, smooth solid surfaces of infinite extent, i.e., fluid confined in a slit pore. Density distributions are calculated here for both hard-sphere and Lennard-Jones fluids. Results obtained from the various models (excluding the van der Waals model which cannot predict structure induced by excluded volume effects) are compared; they are also held up against results from computer simulations of confined fluids.[15,16]

The theories are compared on two levels. The first is based on the form of the coarse-graining weighting functions. In free energy theory, the choice of weighting functions identifies particular model functionals. The models are also compared on the basis of the equation of state used to predict the thermodynamic properties of the hard-sphere reference fluid. The choice of equation of state identifies particular versions of each model.

A. Governing equations

The density of fluid confined in a slit pore varies only in the direction normal to the solid surfaces. Hence, the governing equations from each model can be reduced to one-dimensional form by integrating over directions parallel to the solid surfaces.

The chemical potential, Eq. (2.17), derived from the generic free energy functional of Sec. II A 1 becomes

$$\begin{aligned}\mu - u^{\text{ext}}(x) &= kT \ln n(x) + \int \frac{\delta \bar{n}^{\sigma}(x')}{\delta n(x)} \mathscr{F}_0[\bar{n}^{\tau}(x')]dx' \\ &+ \int \frac{\delta \bar{n}^{\tau}(x')}{\delta n(x)} \bar{n}^{\sigma}(x') \mathscr{F}_0'[\bar{n}^{\tau}(x')]dx' \\ &+ \int n(x)\Phi_x^{\text{att}}(|x-x'|)dx', \end{aligned} \tag{4.1}$$

where

$$\Phi_x^{\text{att}}(|x|) \equiv \int\int \Phi^{\text{att}}(|\mathbf{r}|)dy\,dz. \tag{4.2}$$

The coarse-grained densities $\bar{n}^{\sigma}(x)$ and $\bar{n}^{\tau}(x)$ are given by

$$\bar{n}^{\sigma}(x) = \int \sigma_x(x-x';\{n\})n(x')dx', \tag{4.3}$$

$$\bar{n}^{\tau}(x) = \int \tau_x(x-x';\{n\})n(x')dx', \tag{4.4}$$

where the reduced weighting functions σ_x and τ_x are defined by

$$\sigma_x(x;\{n\}) \equiv \int\int \sigma(\mathbf{r};\{n\})dy\,dz, \tag{4.5}$$

$$\tau_x(x;\{n\}) \equiv \int\int \tau(\mathbf{r};\{n\})dy\,dz. \tag{4.6}$$

The reduced weighting functions corresponding to the free energy models discussed in Sec. II are the generalized van der Waals model:

$$\begin{aligned}\sigma_x(x) &= \delta(x), \\ \tau_x(x) &= \frac{3}{4d^3} H(d-|x|)(d^2-x^2); \end{aligned} \tag{4.7}$$

generalized hard-rod model:

$$\begin{aligned}\sigma_x(x) &= \frac{1}{d} H\left(\frac{d}{2} - |x|\right), \\ \tau_x(x) &= \frac{6}{d^3} H\left(\frac{d}{2} - |x|\right)\left[\left(\frac{d}{2}\right)^2 - x^2\right]; \end{aligned} \tag{4.8}$$

Tarazona model:

$$\begin{aligned}\sigma_x(x-x';\{n\}) &= \delta(x-x'), \\ \tau_x(x-x';\{n\}) &= \omega_{0_x}(x-x') + \omega_{1_x}(x-x')\bar{n}^{\tau}(x) \\ &\quad + \omega_{2_x}(x-x')\bar{n}^{\tau}(x)^2; \end{aligned} \tag{4.9}$$

where

$$\omega_{0_x}(x) = \frac{3}{4d^3} H(d-|x|)(d^2-x^2), \tag{4.10a}$$

$$\begin{aligned}\omega_{1_x}(x) &= H(2d-|x|)H(|x|-d)2\pi\left[0.288d(2d-|x|) - \left(\frac{0.924}{2}\right)(4d^2-|x|^2) + \left(\frac{0.764}{3d}\right)(8d^3-|x|^3)\right. \\ &\quad \left. - \left(\frac{0.187}{4d^2}\right)(16d^4-|x|^4)\right] + H(d-|x|)2\pi\left\{\frac{0.475}{2}(d^2-|x|^2) - \frac{0.648}{3d}(d^3-|x|^3)\right. \\ &\quad \left. + \frac{0.113}{4d^2}(d^4-|x|^4) + d^2\left[0.288 - \frac{3}{2}(0.924) + \frac{7}{3}(0.764) - \frac{15}{4}(0.187)\right]\right\}, \end{aligned} \tag{4.10b}$$

$$\begin{aligned}\omega_{2_x}(x) &= H(d-|x|)\frac{10\pi^2 d^3}{144}\left[3(d^2-|x|^2)\right. \\ &\quad \left. - \frac{4}{d}(d^3-|x|^3) + \frac{5}{4d^2}(d^4-|x|^4)\right]. \end{aligned} \tag{4.10c}$$

When density varies only in the x direction, the Yvon–Born–Green equation, Eq. (2.45), can be integrated from 0 to x to obtain

$$\begin{aligned}\kappa - u^{\text{ext}}(x) &= kT \ln n(x) + \int n(x')\Phi^{\text{att}}(|x-x'|)dx' \\ &\quad + 2\pi kT \int_0^x dx'' \int_{-d}^{+d} dx'\, x' n(x'+x'') \\ &\quad \times g_0^{\text{hs}}[\bar{n}(x''+\tfrac{1}{2}x')], \end{aligned} \tag{4.11}$$

where

$$\bar{n}(x) = \frac{6}{d^3}\int H\left(\frac{d}{2} - |x-x'|\right) \times\left[\left(\frac{d}{2}\right)^2 - (x-x')^2\right] n(x')dx'. \tag{4.12}$$

The quantity κ is a constant of integration and is a thermodynamic field variable. Physically, it represents a mechanical potential of the system.

Confined fluid can of course be in equilibrium with bulk fluid which acts as a reservoir supplying particles to the slit-pore. Such bulk fluid is necessarily at the same chemical potential as the confined fluid. However, the normal stress exerted by the confined fluid on the solid walls is not in general equal to the bulk pressure of the reservoir fluid.

Whereas the free energy theories yield an equation describing the density distribution at chemical equilibrium, the

YBG equation is an expression of mechanical equilibrium in the fluid.[33] As such, the chemical potential is not known in the YBG formalism. Thus free energy models are thus more naturally applicable to grand canonical systems, wherein a bulk reservoir fluid, or equivalently a chemical potential, can be identified. Typical applications of this kind are colloidal interactions in dispersed systems, and adsorption of fluid components in a porous medium.

The basis of comparison we use to examine both the YBG and free energy models is the prediction of the density distribution at a specified mean pore density. The mean pore density, n_{pore}, of confined fluid in a slit-pore of width L with solid walls located at $\pm L/2$ is

$$n_{\text{pore}} = \frac{1}{L}\int_{-L/2}^{L/2} n(x)dx. \tag{4.13}$$

When applying free energy models to confined fluid at a specified mean pore density, the chemical potential μ becomes an additional unknown and must be solved for. Similarly, when the YBG model is applied to such systems, the mechanical potential κ must be solved for.

B. Computational method

Equilibrium density distributions predicted by the free energy models are solutions of Eq. (4.1). Inputs for each particular model are the forms of the weighting functions and the excess hard-sphere free energy per particle as determined from the equation of state used to model the hard-sphere reference fluid.

The density distributions predicted by the YBG theory are solutions of Eq. (4.11). The homogeneous hard-sphere pair correlation function, evaluated at contact, must be specified from the equation of state which is used to model the hard-sphere reference fluid.

Additional inputs required of all models are the fluid–fluid and solid–fluid potentials which govern the behavior of the system to be investigated. The hard-sphere potential does not appear explicitly in any of the governing equations for fluid density. On the other hand, all models presented treat the attractive interactions by the mean-field approach.

In both the free energy and YBG models, the effect of the solid surfaces at $x = \pm L/2$ is treated as an external potential acting on the fluid. The total external potential is the sum of the individual potentials exerted by each wall:

$$u^{\text{ext}}(x) = u_{\text{wall}}\left(\frac{L}{2} - x\right) + u_{\text{wall}}\left(\frac{L}{2} + x\right). \tag{4.14}$$

To facilitate solving the governing equations of fluid density, $n(x)$ was replaced by the variable $Y(x)$,

$$Y(x) \equiv n(x)\exp[u^{\text{ext}}(x)/kT], \tag{4.15}$$

because this is a more slowly varying function of x in the interval $-L/2 < x < L/2$. The domain of interest, $-L/2 < x < L/2$, was discretized uniformly and trapezoidal rule was used to evaluate the integrals. The governing equation of fluid density becomes a system of nonlinear, coupled, algebraic equations for the nodal values of Y. We chose Newton's method to solve for the unknowns; it is probably the most efficient method available. We employed a mesh size of $0.0125d$ in the calculations reported here.

TABLE I. Units used in computations and presentation of results.

Quantity	Units
Distance	d
Wall separation	d
Density	d^{-3}
Pressure	kTd^{-3}
Particle–wall diameter σ_ω	d
Particle–particle energy ϵ	kT
Particle–wall energy ϵ_ω	kT
Chemical potential μ	kT
Mechanical potential κ	kT

The units used for the quantities discussed in subsequent sections are given in Table I. The computer program used for all the models discussed here was written in FORTRAN, and an interactive version of the code is listed elsewhere.[34]

C. Hard-sphere fluid confined between hard walls

A simple, yet telling, standard of comparison of all models is the prediction of the density distribution of hard spheres confined between hard walls. This comparison reveals the ability of each model to predict structure induced by excluded volume effects.

The fluid particles interact solely with a hard-sphere potential, given by Eq. (2.2). The external potential due to hard walls located at $\pm L/2$ is given by

$$\begin{aligned} u_{\text{ext}}(x) &= \infty, \quad |x| > \frac{L}{2} - \frac{d}{2}, \\ &= 0, \quad |x| \leqslant \frac{L}{2} - \frac{d}{2}, \end{aligned} \tag{4.16}$$

where d is the effective hard-sphere diameter.

We use the models discussed in Sec. II to predict the density distribution of a hard-sphere fluid confined between hard walls. To compare with the Monte Carlo simulation results of Snook and Henderson,[15] we calculate the density distribution of fluid confined between hard walls separated a distance $L = 9.74d$, at a mean pore density of $0.8978d^{-3}$. For this density, values of the field variables, i.e., chemical potential in the free energy approach and the mechanical potential in the YBG approach, are given in Table II for each model fluid.

TABLE II. Thermodynamic parameters for hard-sphere fluid between walls separated $9.74d$. The mean pore density is $0.897d^{-3}$ for all fluids compared.

Model	μ or κ	P_N
GVDW–Clausius	9.77	7.73
GVDW–Carnahan/Starling	11.12	7.32
GHR–Clausius	19.50	16.54
GHR–Carnahan/Starling	15.81	11.29
TRZ–Clausius	14.95	12.35
TRZ–Carnahan/Starling	15.67	11.11
YBG–Clausius	2.85	17.28
YBG–Carnahan/Starling	2.39	10.88
Monte Carlo (Ref. 15)	···	10.30

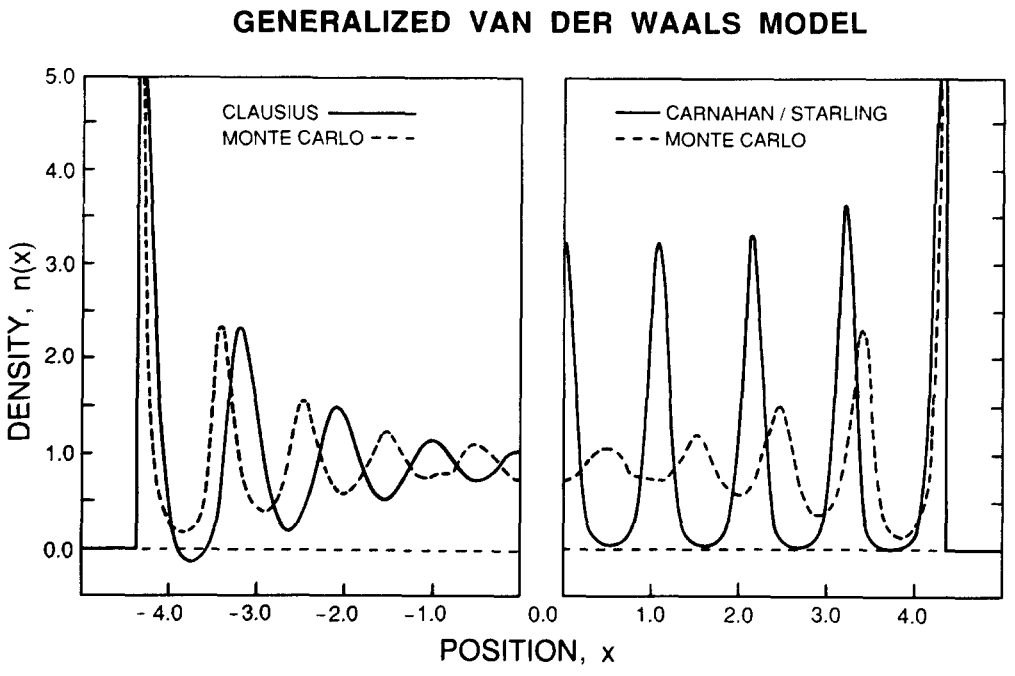

FIG. 1. Comparison of density profiles predicted by the generalized van der Waals model with Monte Carlo simulation (Ref. 15) of confined hard-sphere fluid.

A characteristic feature of the density profile of fluid confined between solid surfaces is the average layer spacing of the density distribution. In a confined fluid, the layer spacing is determined by a competition between the intrinsic spacing characteristic of the semiconfined fluid, i.e., fluid next to a single solid surface, and the packing and symmetry constraints induced by the presence of a second confining surface. Thus, the layer spacing predicted by a given model can vary with position in the pore, and is, in general, a function of pore width. Because walls spaced a distance $9.74d$ interact scarcely at all, the layer spacing of the confined fluid near the walls is almost the same as the intrinsic layer spacing of the semiconfined fluid. For sake of comparison, we can estimate for each model the intrinsic layer spacing from the average spacing between the first three density layers. The Monte Carlo simulation predicts an average layer spacing of $0.94d$.

When fluid is confined between hard walls, the normal pressure in the pore is related to the magnitude of the density at each wall:

$$P_N = kTn(0). \tag{4.17}$$

At the given mean pore density, the Monte Carlo simulation predicts a normal pressure in the pore of $10.3\ kTd^{-3}$. The normal pressure predicted by each model is also listed in Table II. Because the walls are essentially noninteracting, the normal pressure of the confined fluid is not significantly different from the pressure of bulk fluid at the prescribed field variables.

Density profiles predicted by the generalized van der Waals model are compared with the Monte Carlo results in Fig. 1; the density distribution from $-L/2$ to 0 is that predicted by the Clausius version of the model and the density distribution from 0 to $L/2$ is that predicted by the Carnahan/Starling version of the model. Both versions of the generalized van der Waals model predict a layer spacing that is consistently greater than one particle diameter throughout the slit pore. The Clausius version predicts an average layer spacing of $1.14d$ (based on the first three layers); the Carnahan/Starling version predicts a similar average spacing of $1.12d$. Both versions of the model underpredict the pressure in the pore, by 25% for the Clausius fluid and by 29% for the Carnahan/Starling fluid.

As mentioned previously, when the Clausius expression for $\mathcal{F}_0(n)$ is used, in the Euler–Lagrange equation of the generalized van der Waals model, regions of negative density are predicted. For this particular choice of $\mathcal{F}_0(n)$, the governing equation, Eq. (4.1), can be rewritten as

$$h(x) = e^{[\mu - u^{\rm ext}(x)]} \times \exp\left\{ -\frac{3}{4} \int_{|x-x'|\leq d} [d^2 - (x-x')^2] \times h(x')dx' \right\}, \tag{4.18}$$

where

$$h(x) \equiv \frac{n(x)}{[1 - \bar{n}^{\tau}(x)d^3]}. \tag{4.19}$$

This transformation reveals that a negative density at any position x is coupled with a coarse-grained density at the same x that is greater than d^{-3}, the close-packed limit. The function $h(x)$, however, is well-behaved at all values of chemical potential.[24]

When the Carnahan/Starling expression for $\mathcal{F}_0(n)$ is used, the generalized van der Waals model predicts density distributions that are everywhere nonnegative. In this case, however, the density distribution becomes stratified at high mean pore density, and this leads to density peaks characteristic of liquid crystals, as shown in Fig. 1. These sharp peaks persist uniformly through the fluid, even when the solid separation is increased to $L = 20d$ at constant chemical poten-

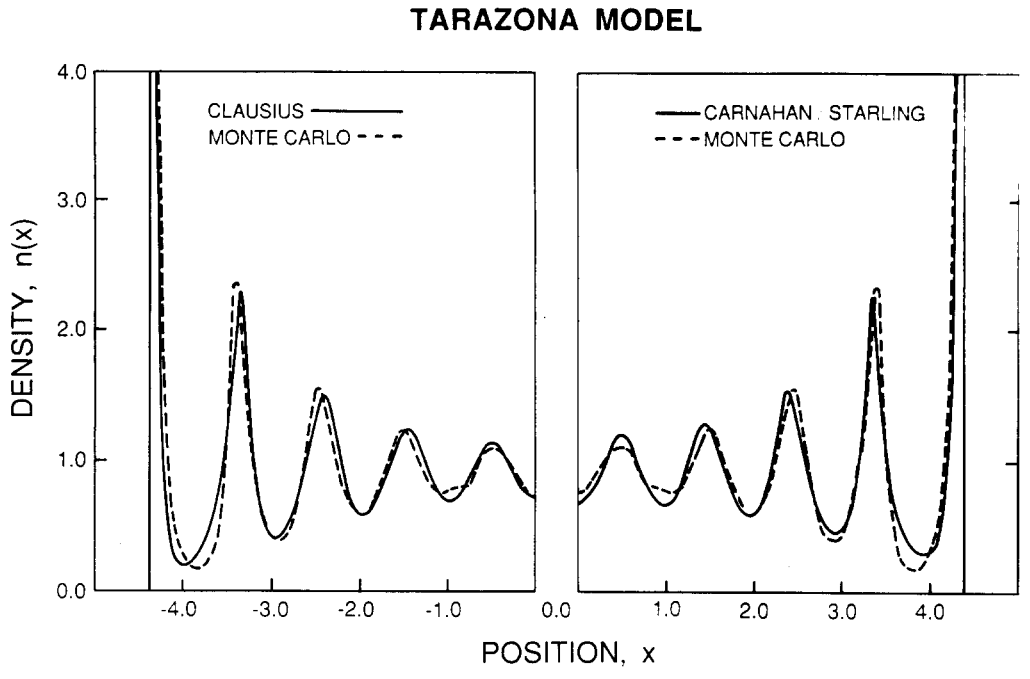

FIG. 2. Comparison of density profiles predicted by the Tarazona model with Monte Carlo simulation (Ref. 15) of confined hard-sphere fluid.

tial. This is clearly in disagreement with the simulation results which predict that the density layering is already weak in the center of the pore at a separation of $9.74d$.

In summary, the Euler–Lagrange equation of the generalized van der Waals model, although the simplest nonlocal free energy functional, does not predict physically realistic structure at high mean pore densities. Furthermore, the qualitative structure of the predicted density profiles is strongly dependent on the equation of state used to specify the excess hard-sphere free energy. The negative densities could be avoided by hunting the minimum of Ω under the physical constraint $n(x) \geqslant 0$.

The Tarazona model, which represents a systematic improvement on the generalized van der Waals model, admits no unphysical solutions at high mean pore density. The density profiles predicted by Clausius and Carnahan/Starling versions of the model are shown in Fig. 2. Of all models considered, the Tarazona model predicts density profiles in closest agreement with the simulation results. Density profiles predicted by the Tarazona model do not depend strongly on the equation of state chosen to model the hard-sphere reference fluid. Both versions of the model predict an average layer spacing of $0.99d$, just slightly larger than the layer spacing predicted by the simulation. The only major difference between the two versions of the model is the normal pressure in the pore: The Carnahan/Starling version pre-

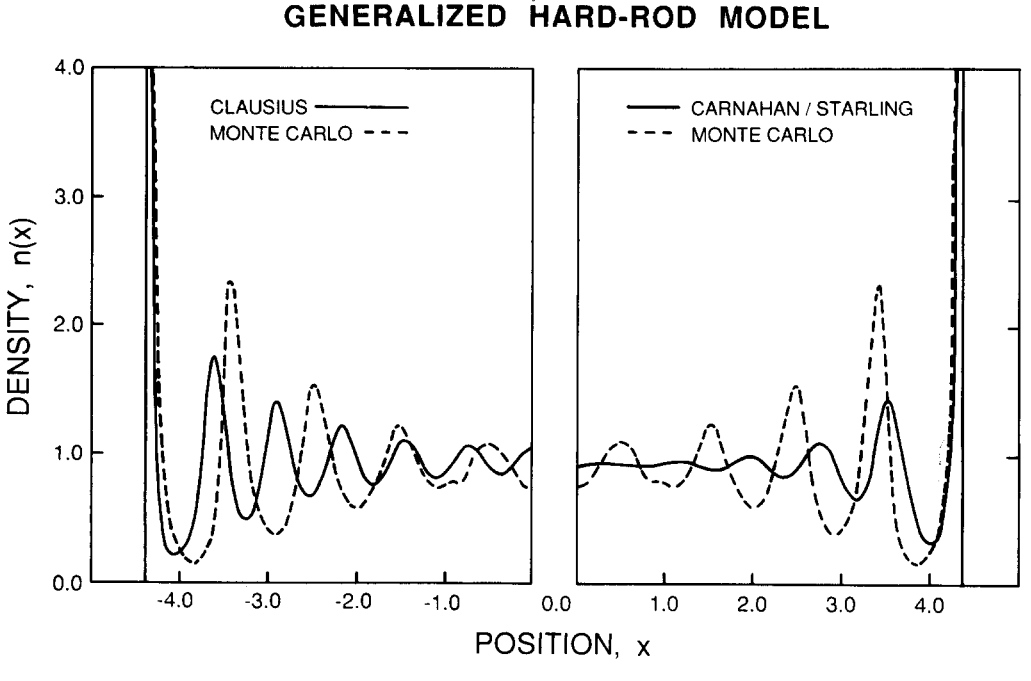

FIG. 3. Comparison of density profiles predicted by the generalized hard-rod model with Monte Carlo simulation (Ref. 15) of confined hard-sphere fluid.

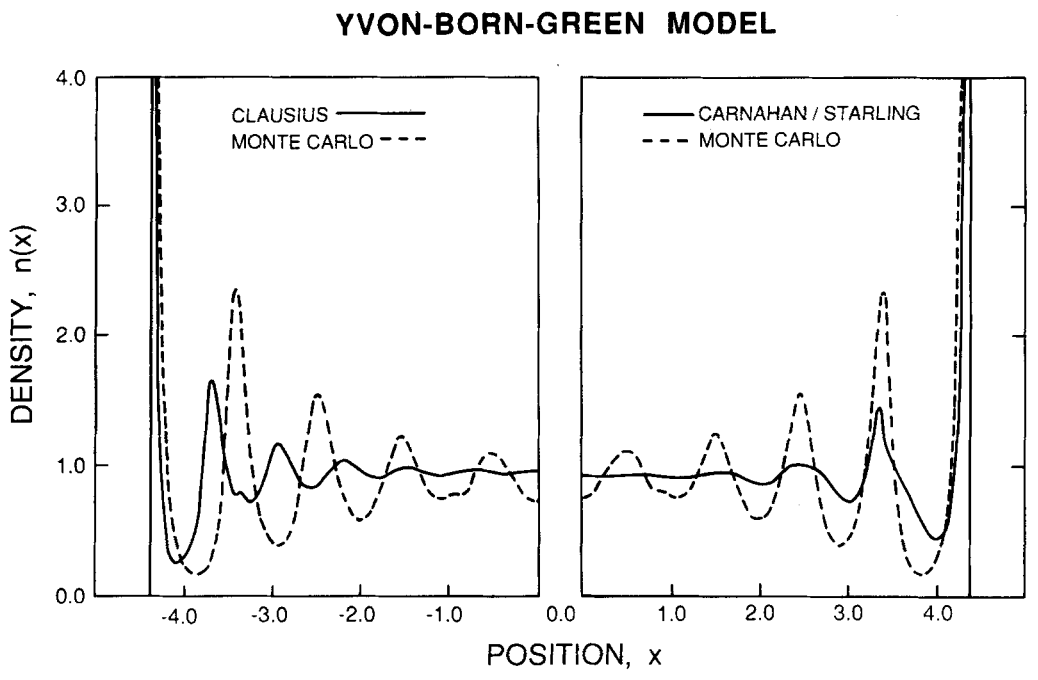

FIG. 4. Comparison of density profiles predicted by the Yvon–Born–Green model with Monte Carlo simulation (Ref. 15) of confined hard-sphere fluid.

dicts a normal pressure in closer agreement with the simulation result (8% high) while the Clausius version overpredicts the pressure by 20%.

Density profiles predicted by the Clausius and Carnahan/Starling versions of the generalized hard-rod model are shown in Fig. 3. Both versions of the model predict density profiles that are physically acceptable, but the profiles are less structured than the density profile observed in the simulation. Both versions of the model also predict average layer spacings that are smaller than the simulation result. The Clausius version predicts an average spacing of $0.74d$; the Carnahan/Starling version predicts an average spacing of $0.81d$, in closer agreement with the simulation. The normal pressure predicted by the Carnahan/Starling version is also in much closer agreement with the simulation result (10% high) than the pressure predicted by the Clausius version of the model (61% high). The density profile of the Clausius fluid is more pronounced and is longer ranged than the density profile of the Carnahan/Starling fluid, owing to the relative difference in pressure.

Density profiles predicted by the Clausius and Carnahan/Starling versions of the YBG equation with the Fischer–Methfessel approximation are shown in Fig. 4. The average layer spacing predicted by the YBG model depends strongly on the equation of state use to model the hard-sphere reference fluid. The average layer spacing predicted by the Clausius version of the YBG model is $0.73d$, which is smaller than the simulation result and similar to that predicted by the Clausius version of the generalized hard-rod model. On the other hand, the average spacing predicted by the Carnahan/Starling version of the YBG model is $0.98d$, in close agreement with the simulation result. As with all other models considered, the normal pressure of the confined Clausius fluid is substantially higher (68% higher than the simulation) than that of the confined Carnahan/Starling fluid (only 6% higher than the simulation). Both versions of the YBG model are poorer than the Tarazona free energy model in predicting the layered structures observed in the computer simulation.

The shape of the density profile predicted by the Clausius version of the YBG model differs qualitatively from those predicted by all the other models considered. This version of the YBG model predicts a region of low density at approximately $1d$ from each hard wall that is composed of two shallow local minima. This feature does not appear in the Carnahan/Starling version of the YBG model.

In summary, of all models considered the Carnahan/Starling version of the Tarazona model gives the best overall performance. This model predicts density profiles in closest agreement with those observed in the Monte Carlo simulation. Furthermore, the normal pressure and average layer spacing estimated by the model are in good agreement with the simulation results. While the Carnahan/Starling version of the YBG model predicts normal pressure and average layer spacing in closest agreement with the simulation results, this model underestimates the degree of density layering that is observed in the simulation.

D. Lennard-Jones fluid confined between Lennard-Jones walls

The models presented in Sec. II are now used to predict the density distribution of Lennard-Jones fluid particles confined between attractive walls, each exerting a Lennard-Jones 10-4-3 potential. Here the models are examined to see how well the predicted profiles agree with those obtained from the molecular dynamics simulation of Magda *et al.*[16]

The external potential exerted on the fluid by Lennard-Jones 10-4-3 walls located at $\pm L/2$ is given by Eq. (4.14)

TABLE III. Thermodynamic parameters for Lennard-Jones fluid between Lennard-Jones walls. The mean pore density at $L = 3d$ is $0.5297d^{-3}$ and at $L = 4d$ it is $0.4811d^{-3}$.

Model	L	μ or κ	P_N
GVDW–Clausius	4.0	−7.40	−1.22
	3.0	−7.73	−0.75
GVDW–Carnahan/Starling	4.0	−4.70	0.04
	3.0	−5.06	0.26
GHR–Clausius	4.0	−4.88	3.69
	3.0	0.27	2.15
GHR–Carnahan/Starling	4.0	−1.46	0.97
	3.0	−0.16	0.84
TRZ–Clausius	4.0	−6.62	−0.96
	3.0	−6.43	−0.35
TRZ–Carnahan/Starling	4.0	−2.99	0.16
	3.0	−2.52	0.54
YBG–Clausius	4.0	−1.32	3.36
	3.0	−1.92	1.88
YBG–Carnahan/Starling	4.0	−3.06	0.16
	3.0	−3.04	0.32
Molecular dynamics[15]	4.0	···	0.38 ± 0.1
	3.0	···	0.49 ± 0.06

with

$$u_{\text{wall}}(x) = 2\pi\epsilon_\omega \left[\frac{2}{5}\left(\frac{\sigma_\omega}{x}\right)^{10} - \left(\frac{\sigma_\omega}{x}\right)^4 - \frac{\sqrt{2}\sigma_\omega^3}{3\left[x + (0.61/\sqrt{2})\sigma_\omega\right]^3}\right], \tag{4.20}$$

where ϵ_ω and σ_ω are characteristic wall–fluid energy and distance parameters.

The fluid particles are assumed to interact with an attractive potential of the form

$$\Phi^{\text{at}}(|\mathbf{r}|) = -4\epsilon\left(\frac{d}{r}\right)^6, \quad |\mathbf{r}| \geqslant d$$
$$= 0, \quad |\mathbf{r}| < d, \tag{4.21}$$

which, after integration over the y–z plane, becomes

$$\Phi_x^{\text{att}}(|x|) = -2\pi\epsilon d^2\left(\frac{d}{x}\right)^4, \quad |x| \geqslant d,$$
$$= -2\pi\epsilon d^2, \quad |x| < d. \tag{4.22}$$

In accordance with the thermodynamic parameters of the simulation of Magda *et al.*,[16] the following values were chosen for the solid–fluid and fluid–fluid parameters used in the models. The particle–particle interaction energy ϵ and the solid–fluid interaction energy ϵ_ω are taken to be $1.21\,kT$. The solid–fluid distance parameter σ_ω is equal to d. Comparisons are made for fluid at a mean pore density of $0.5297d^{-3}$ confined between walls separated $3d$, and for fluid at a mean pore density of $0.4811d^{-3}$ confined between walls separated $4d$. Values of the controlling field variable, chemical potential or mechanical potential, for each model fluid are listed in Table III.

The normal pressure exerted by the confined fluid on the solid walls can be calculated directly from the density distribution. For walls with continuous potentials, the nor-

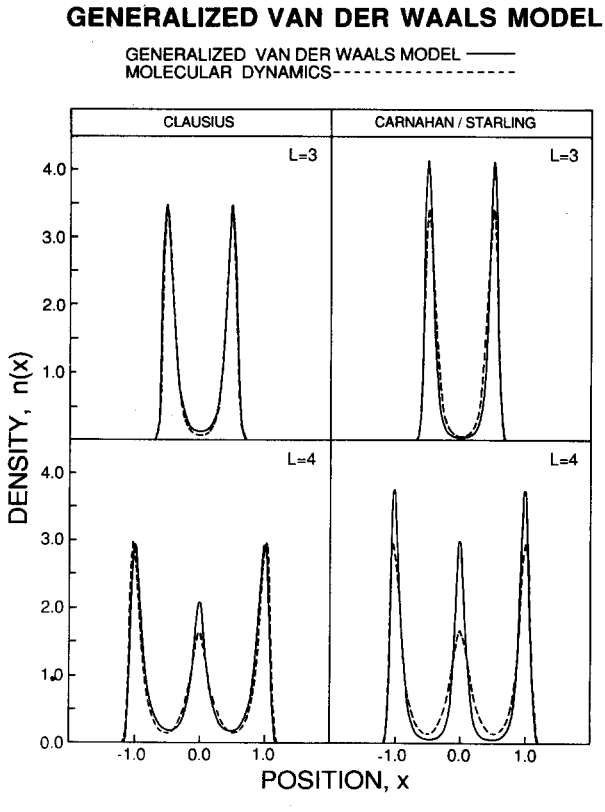

FIG. 5. Comparison of density profiles predicted by the generalized van der Waals model with molecular dynamics simulations (Ref. 16) of confined Lennard-Jones fluid.

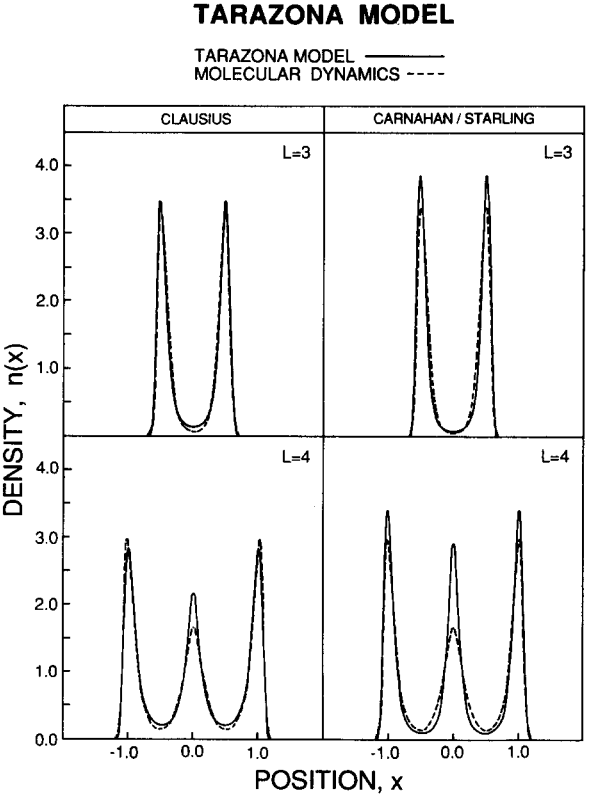

FIG. 6. Comparison of density profiles predicted by the Tarazona model with molecular dynamics simulations (Ref. 16) of confined Lennard-Jones fluid.

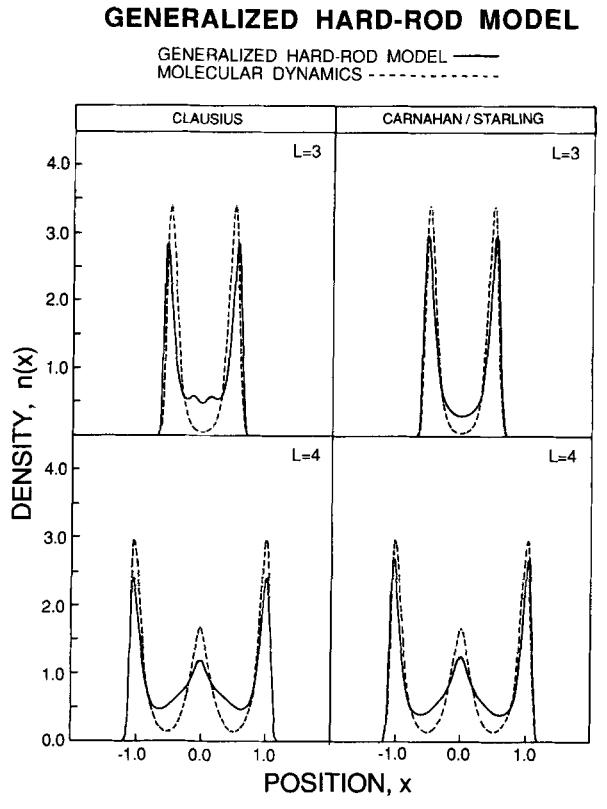

FIG. 7. Comparison of density profiles predicted by the generalized hard-rod model with molecular dynamics simulations (Ref. 16) of confined Lennard-Jones fluid.

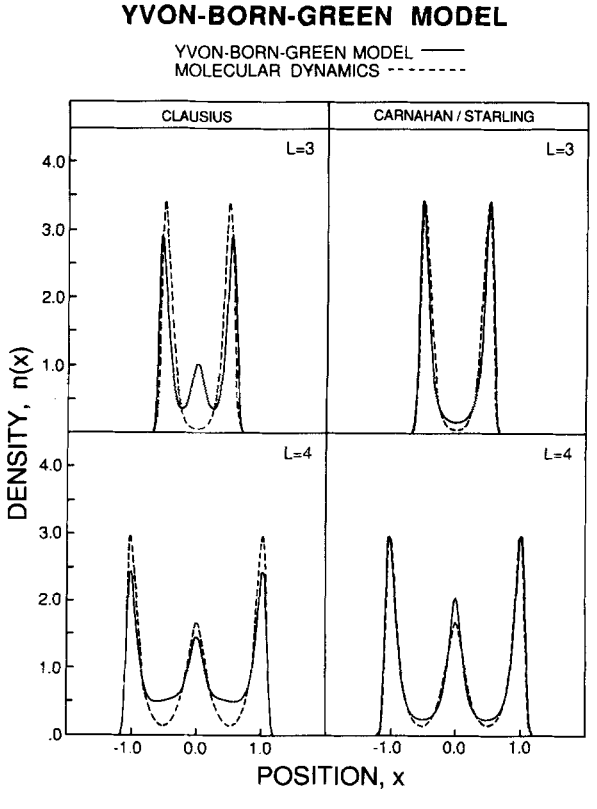

FIG. 8. Comparison of density profiles predicted by the Yvon–Bron–Green model with molecular dynamics simulations (Ref. 16) of confined Lennard-Jones fluid.

mal pressure is given by[35]

$$P_N = -\frac{1}{2}\int_{-L/2}^{L/2} \frac{du^{\text{ext}}(x')}{dx'} n(x')\, dx'. \tag{4.23}$$

Values of P_N as determined from the density distributions are also reported in Table III.

Molecular dynamics simulation results of Magda *et al.*[16] are compared with density profiles predicted by the generalized van der Waals model in Fig. 5, the Tarazona model in Fig. 6, and the generalized hard-rod model in Fig. 7. Figure 8 compares the simulation results with the predictions of the YBG model.

Both versions of the generalized van der Waals model predict density profiles that are similar to those predicted by the corresponding versions of the Tarazona model. The Clausius version of each model predicts primary density peaks adjacent to each wall that are within 2% of the simulation results. At the larger pore width, both models overpredict the middle density peak, by as much as 25% for the generalized van der Waals model and 30% for the Tarazona model.

The Carnahan/Starling versions of both models consistently overpredict the magnitudes of all density peaks. At $L = 3d$, the generalized van der Waals model predicts primary density peaks 20% higher than those observed in the simulation. The Tarazona model overpredicts the height of these peaks by 13%. At $L = 4d$, the generalized van der Waals model overpredicts the primary peaks by 26% and the middle peak by 80%. The Tarazona model does only slightly better, overpredicting the primary peaks by 15% and the middle peak by 74%.

Although the density profiles predicted by the Clausius versions of both models are in better agreement with the simulation results, the normal pressure is in both cases better predicted by the Carnahan/Starling versions of the models (see Table III). The disagreement between simulation and the predictions are smallest for the Tarazona model.

At the smaller pore width, both the Clausius version of the generalized hard-rod model and the Clausius version of the YBG model predict density profiles that are qualitatively different from those observed in the simulation. Both of these models predict an intrinsic density layer spacing in a semi-confined fluid that is significantly less than one effective hard-sphere diameter. Thus instead of the two-layered configuration predicted by the simulation, the generalized hard-rod Clausius model predicts a four-layered structure while the YBG–Clausius model predicts a three-layered structure.

At the larger pore width, the Clausius version of the generalized hard-rod model and Clausius version of the YBG model predict density profiles that are in qualitative agreement with the simulation results, although both models underestimate the magnitudes of density peaks. The generalized hard-rod model underpredicts the magnitude of the primary density peaks by as much as 20% and the middle peak by 30%. The YBG model underestimates the primary density peaks by 18% and the middle peak by 14%. The pressure estimated by both the Clausius generalized hard-rod model and the Clausius–YBG model are in very poor agreement with the simulation results.

Unlike the Clausius versions, the Carnahan/Starling versions of the generalized hard-rod model and the YBG model predict density profiles in qualitative agreement with those observed in the simulations. The generalized hard-rod model, however, still underestimates the degree of molecular structuring in the fluid. At $L = 3d$, the generalized hard-rod model underpredicts the height of the primary density peaks by 14%. At $L = 4$, it underpredicts the primary density peaks by 10% and the middle peak by 25%. On the other hand, of all models considered, the Carnahan/Starling version of the YBG model predicts density profiles in closest agreement with the simulation results. The primary peaks are within 1% of the simulation results for both $L = 3d$ and $L = 4d$. At the larger pore width, the YBG model overpredicts the middle peak by only 21%. The normal pressures predicted by the Carnahan/Starling version of the YBG model are in much closer agreement with the simulation results than the pressures predicted by the Carnahan/Starling version of the generalized hard-rod model.

In summary, pressures predicted by the Carnahan/Starling versions of the models are in all cases in better agreement with the simulation results than are the predictions of the corresponding Clausius versions. Although the Carnahan/Starling version of the Tarazona model tends to overpredict the heights of the density peaks observed in the molecular dynamics simulations, it gives the best estimates of pressure. The Carnahan/Starling version of the YBG model predicts density profiles in closest agreement with the simulations and pressures that are almost as good as those predicted by the Tarazona model.

V. SUMMARY

Several approximate density functional models of inhomogeneous fluid have been examined. Each model attempts to account for the nonlocal effects arising from the finite size of fluid particles by incorporating coarse-grained densities. These coarse-grained densities are functionals of the local density distribution. They are most generally defined as weighted averages of the local density in a domain of size comparable to the range of molecular interactions. The nonlocal weighting functions used to define the coarse-grained densities distinguish the various models. All models require as input the equation of state of a homogeneous fluid evaluated at a local coarse-grained density. Two mean field equations of state were used, one based on a Carnahan/Starling hard-sphere reference fluid and the other based on a Clausius hard-sphere reference fluid.

The generalized van der Waals model is the simplest free energy density functional model that incorporates a coarse-grained density. However, this model fails to predict physically reasonable density distributions at high mean pore density, regardless of the equation of state used to model the hard-sphere reference fluid. The nonlocal weighting function employed in the generalized van der Waals model is generated as the lowest order term in the series expansion used to construct the nonlocal weighting function employed in the Tarazona Model. The Tarazona model, which keeps two more terms in the expansion, admits no unphysical solutions at high mean pore density. As would be expected, density profiles predicted by the generalized van der Waals model are in close agreement with those predicted by the Tarazona model at small mean pore densities, although the prediction of pressure is not as good.

The Tarazona model based on the Carnahan/Starling equation of state gives the best overall performance. This model predicts pressures in close agreement with computer simulation for both hard-sphere and Lennard-Jones confined fluids. Of all models considered, the Carnahan/Starling version of the Tarazona model predicts density profiles for confined hard-sphere fluid in closest agreement with the Monte Carlo results of Snook and Henderson,[15] and density profiles for confined Lennard-Jones fluid in good qualitative agreement with the molecular dynamics results of Magda *et al.*[16]

The Carnahan/Starling version of the YBG model also delivers a strong performance. For confined hard-sphere fluid, this model predicts normal pressure and average layer spacing in closest agreement with the Monte Carlo results, although it underpredicts the degree of molecular structuring in the fluid. For confined Lennard-Jones fluid, the Carnahan/Starling version of the YBG model predicts density profiles in closest agreement with the molecular dynamics results and predicts the pressure almost as well as the Tarazona model.

The generalized hard-rod model and the YBG model are based on intuitive extensions of the rigorous one-dimensional hard-rod theory to three dimensions. While these models fail to agree quantitatively with simulation results, they capture the qualitative behavior of confined hard-sphere and Lennard-Jones fluids. Both models retain much of the mathematical and physical simplicity enjoyed by the generalized van der Waals model, but do not fail at high mean pore density. They might be especially useful for qualitative study of confined fluid mixtures for which the complexity of the Tarazona approach becomes more formidable.

ACKNOWLEDGMENTS

The authors are grateful to the ACS Petroleum Research Fund, the National Science Foundation, the Department of Energy, and the Minnesota Supercomputer Institute for financial support of this research. We also would like to acknowledge the American Association of University Women for a doctoral dissertation fellowship awarded to T.K.V.

[1] J. D. van der Waals and Ph. Kohnstamm, *Lehrbuch der Thermodynamik* (Mass and van Suchtelen, Leipzig, 1908), Vol. 1.
[2] For a discussion of the history of the development of functional theory in statistical mechanics, see G. Stell, in *The Equilibrium Theory of Classical Fluids*, edited by H. L. Frisch and J. L. Lebowtiz (Benjamin, New York, 1964), pp. II71–II226.
[3] J. K. Percus, in *The Equilibrium Theory of Classical Fluids*, edited by H. L. Frisch and J. L. Lebowitz (Benjamin, New York, 1964), pp. II30–II70.
[4] V. Bongiorno and H. T. Davis, Phys. Rev. A **12**, 2213 (1975).
[5] V. Bongiorno, L. E. Scriven, and H. T. Davis, J. Colloid Interface Sci. **57**, 462 (1976).
[6] R. Evans, Adv. Phys. **28**, 143 (1979).
[7] P. Tarazona, M. M. Telo da Gama, and R. Evans, Mol. Phys. **49**, 283, 301 (1983).
[8] G. F. Teletzke, L. E. Scriven, and H. T. Davis, J. Chem. Phys. **78**, 550 (1983).

[9]H. T. Davis, R. E. Benner, L. E. Scriven, and G. F. Teletzke, in *Surfactants in Solution*, edited by K. L. Mittal and P. Bothorel (Plenum, New York, 1986), Vol. 6, pp. 1485–1524.
[10]B. C. Freasier, and S. Nordholm, J. Chem. Phys. **79**, 4431 (1983).
[11]J. Fischer and M. Methfessel, Phys. Rev. A **22**, 2836 (1980).
[12]A. Robledo and C. Varea, J. Stat. Phys. **26**, 513 (1981).
[13]J. Fischer and U. Heinbuch, J. Chem. Phys. **88**, 1909 (1988).
[14]J. K. Percus, J. Stat. Phys. **15**, 505 (1976).
[15]I. K. Snook and D. Henderson, J. Chem. Phys. **68**, 2134 (1978).
[16]J. J. Magda, M. V. Tirrell, and H. T. Davis, J. Chem. Phys. **83**, 1888 (1985).
[17]H. T. Davis and L. E. Scriven, Adv. Chem. Phys. **49**, 357 (1982).
[18]J. K. Percus, J. Chem. Phys. **75**, 1316 (1981).
[19]N. F. Carnahan and K. E. Starling, J. Chem. Phys. **51**, 635 (1969); **53**, 600 (1970).
[20]S. Nordholm, M. Johnson, and B. C. Freasier, Aust. J. Chem. **33**, 2139 (1980).
[21]M. Johnson and S. Nordholm, J. Chem. Phys. **75**, 1953 (1981).
[22]P. Tarazona and R. Evans, Mol. Phys. **52**, 847 (1984).
[23]M. A. Hooper and S. Nordholm, J. Aust. Chem. **34**, 1809 (1981).
[24]T. K. Vanderlick, L. E. Scriven, and H. T. Davis, Phys. Rev. A **34**, 5130 (1986).
[25]P. Tarazona, Phys. Rev. A **31**, 2672 (1985).
[26]W. A. Curtin and N. W. Ashcroft, Phys. Rev. A **32**, 2909 (1985).
[27]T. F. Meister and D. M. Kroll, Phys. Rev. A **31**, 4055 (1985).
[28]P. Tarazona, U. Marini Bettolo Marconi, and R. Evans, Mol. Phys. **60**, 573 (1987).
[29]J. Yvon, *Actualities Scientifique et Industrial* (Herman et Cie, Paris, 1935).
[30]M. Born and H. S. Green, *A General Kinetic Theory of Liquids* (Cambridge, London, 1949).
[31]H. T. Davis, J. Chem. Phys. **85**, 6808 (1986).
[32]T. K. Vanderlick, L. E. Scriven, and H. T. Davis, J. Chem. Phys. **85**, 6699 (1986).
[33]B. Carey, L. E. Scriven, and H. T. Davis, J. Chem. Phys. **69**, 5040 (1978).
[34]T. K. Vanderlick, Ph.D. thesis, University of Minnesota, 1988.
[35]I. K. Snook and W. van Megen, J. Chem. Phys. **70**, 3099 (1979).